2014-2015 NASA Space Grant

Midwest High-Power Rocketry Competition

Post-Flight Performance Report

University of Minnesota Senior Design Team

Team: Space Cowboys

Peter Brackin Sean Conway

Scott Gleason John Kregness

Sean Moore Logan Rowell

Zack Thompson

Course: AEM 4333

Faculty Adviser: Professor James Flaten

May 29th, 2015

Table of Contents

Rocket Operation Assessment

Flight Anomalies Analysis

The anomalies observed from the first and second flights regard the recovery parachute of the dart and the ejection of the parachute, respectively. In the first flight, the parachute was deployed after apogee, as seen in Figure 4, but the parachute did not open. The parachute was unable to open because the shroud lines were tangled for the duration of the descent. The state of the parachute was observable on retrieval of the dart. In order to prevent this from happening in later flights, a new parachute folding technique was used. Instead of wrapping the parachute with the shroud lines to decrease packing volume, the parachute was folded around the shroud lines, which were folded neatly inside the parachute. While this slightly increased packing volume, the shroud lines were less likely to become tangled.

The dart did not pass the flyable condition requirement following the first flight. On landing, the dart’s boat tail was sheared at an epoxy point and the main tube of the dart suffered some delamination in the recovery section. The recovery section of the dart was not repaired, but the boat tail section was epoxied into flight-ready position.

An ejection failure was observed in the second flight, which prevented the parachute from being deployed. Upon retrieval of the dart, the piston used for ejecting the parachute had appeared to be stuck inside the main tube. It was predicted that the piston may have caught on some debris, such as epoxy or donut glaze residue, or the delaminated portion of the main tube. This may have been prevented if the recovery section was inspected and cleaned of debris with a clean towel or napkin and if the ejection charge was slightly increased in mass.

Propulsion System Assessment

Each Cesaroni I445 motor used for launch was inspected for bubbles in the grain. The motor ejections for the first and second flights were adjusted to 11 and 12 seconds, respectively, after burnout. Judging from Figure 3, the acceleration of the boosted-dart performed as predicted.

Flight Path Assessment

Figures 6 and 7 of the 3-axis motion indicate that the dart maintained a trajectory that deviated little in the transverse directions. After apogee, sway can be observed in the dart's motion as it plummets to the ground.

Recovery System Assessment

The electronics used for recovery operated as intended. However, the piston ejection and the parachute experienced different failures in separate flights. In the first flight, the parachute had been pre-wrapped with shroud lines keeping the parachute tight and compact. The period of time since being wrapped caused the parachute and shroud lines to be settled into its failure state. In the second flight, the piston ejection experienced a failure due to airframe irregularities, debris, or residue along the piston's exit path.

Rocket Location & Recovery Analysis

For both launches, the booster and dart were both recovered in a radius of approximately 500-1000 feet from the launch pad. The booster was tracked by sight while the dart was tracked by radio frequency. The booster was recovered in flyable condition for both flights, but the dart suffered minor damage after the first flight and critical damage after the second flight.

Pre- & Post- Launch Procedure Assessment

A checklist was used to follow the pre-launch and post-launch procedures in sequence. The team experienced some deviation in the checklist when trying to correct minor faults with the avionics bays of both the booster and the dart, but would proceed with the correct checklist sequence after their correction. A major deviation that was unaccounted for in the first flight was the wrapping of the parachute. Although the parachute was packed, as intended, neglecting to rewrap the parachute caused the parachute to fail in flight. After retrieving the booster and dart, the avionics were shut off in the prescribed order and all available data was processed.

Actual vs. Predicted Performance

The following Table 1 is a summary of the performance characteristics of the boosted-dart's first flight.

Operation (determined by RSO or designee)		
	Launch	Yes
	Parachute Deployment	Yes
	Recovered	Yes
	Determined to be in flyable condition	No

	Predicted	Actual
Maximum Altitude [ft.]	3912	4273
Peak Velocity [ft/s]	646.7	575.6
Peak Acceleration [ft/s^2]	23.15	22.16
Booster Apogee [ft]	2603	2888
Dart Apogee [ft]	3912	4273
Apogee Separation [ft]	1309	1385

Table 1. Performance characteristics of boosted-dart.

Using the data from the Raven3 altimeter and BMP180 devices aboard the dart and booster, respectively, the altitudes of the dart and booster are shown in Figure 1. The actual altitudes of the booster and dart were both greater than predicted. This is justified because predicted performances are determined from 15% deviation from ideal fair-weather conditions with negligible weather-cocking to account for approximately 15 mile per hour crosswinds. As a disclaimer, this is not an ideal adjustment that will accurately reflect all of the altitude, velocity, and acceleration curves. Although the velocity and acceleration curves seen in Figures 2 and 3, suggest that the dart would have a smaller altitude than predicted, Figure 2 shows that the deceleration after burnout is smaller than predicted. The difference in apogees for either set of results were relatively accurate and only differed by 76 feet (see Table 1).

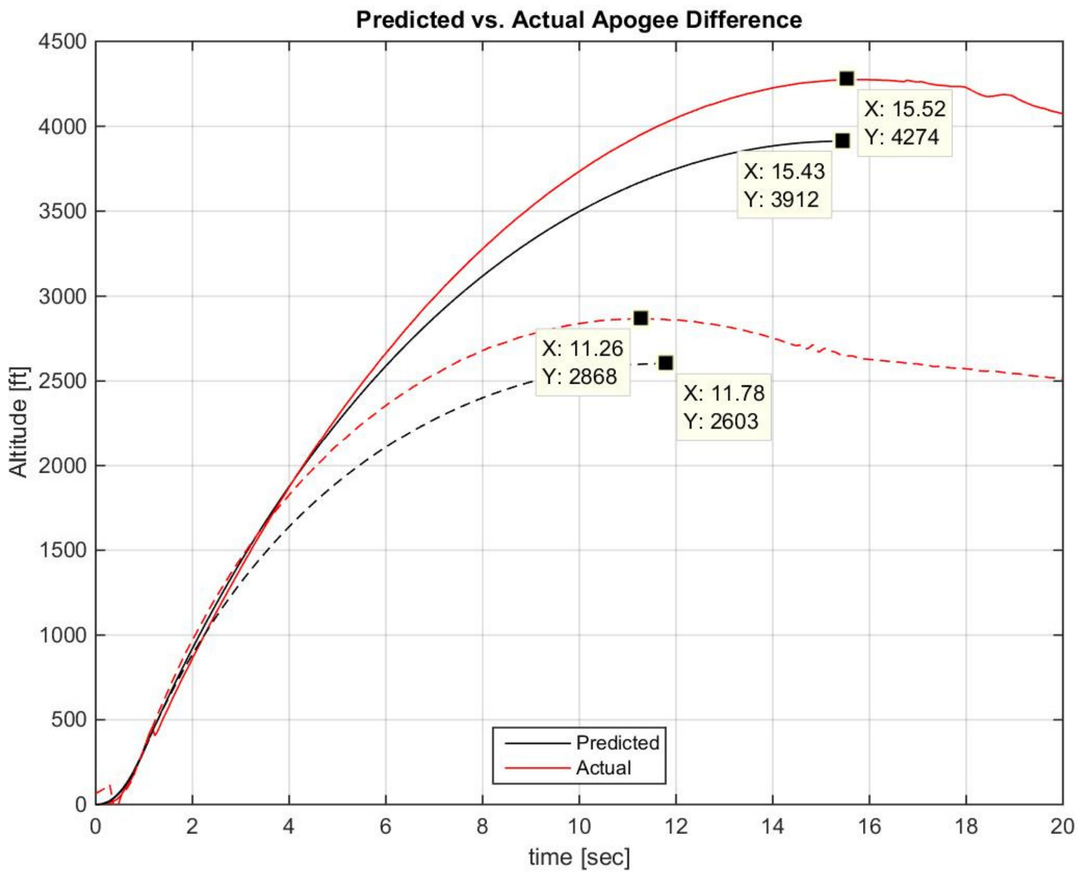

Figure 1. Altitude curves of the booster and dart sections through boosting and coasting phases. The solid line variants indicate the dart altitude and the dashed line variants indicate the booster altitude.

The data for the velocity and acceleration curves seen in Figures 2 and 3 were taken from the Raven3 altimeter in the dart. Comparing the actual and predicted results shows that the dart underperformed in the boosting phase for both the velocity and acceleration curves. Although the predicted cases account for less than ideal weather, the predicted drag on the dart must be an over estimate, while the predicted drag on the boosted-dart combination would an under estimate. With the exception of the booster altitude, this would explain why the dart achieves a higher altitude than predicted at a slower velocity and acceleration.

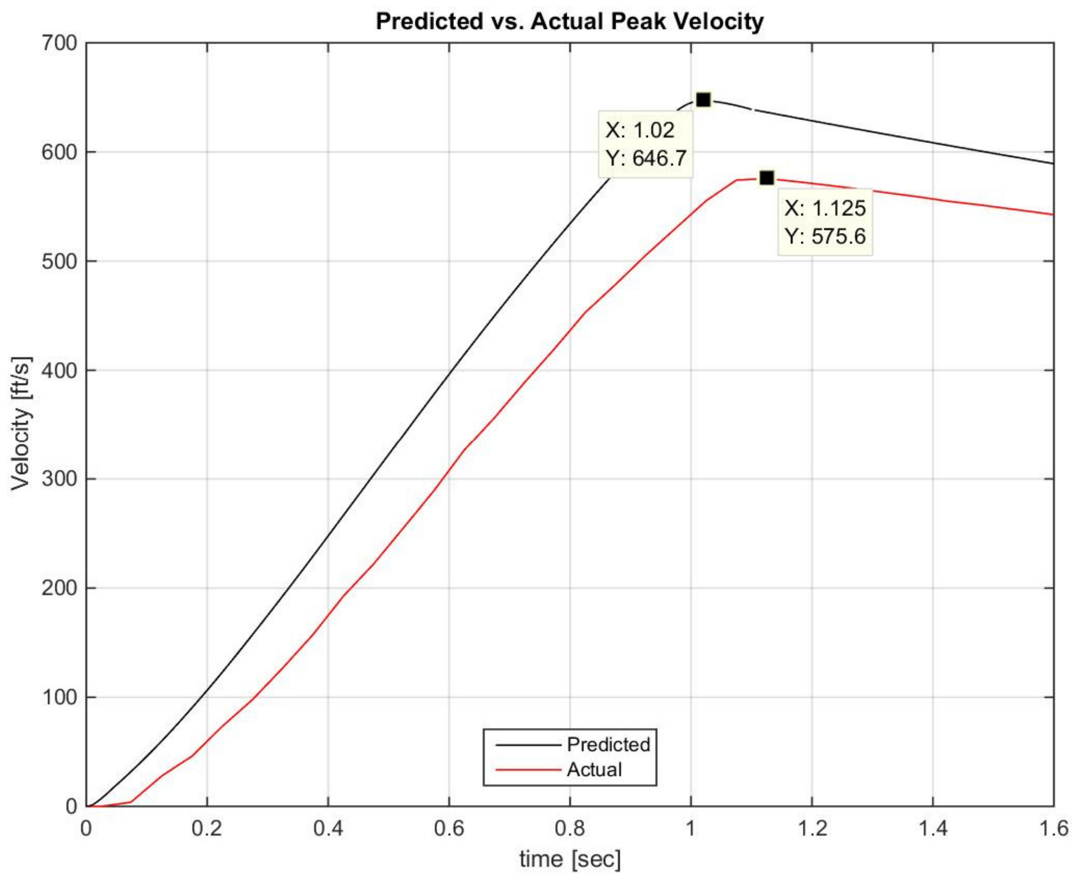

Figure 2. Velocity curve of the dart during boosting phase.

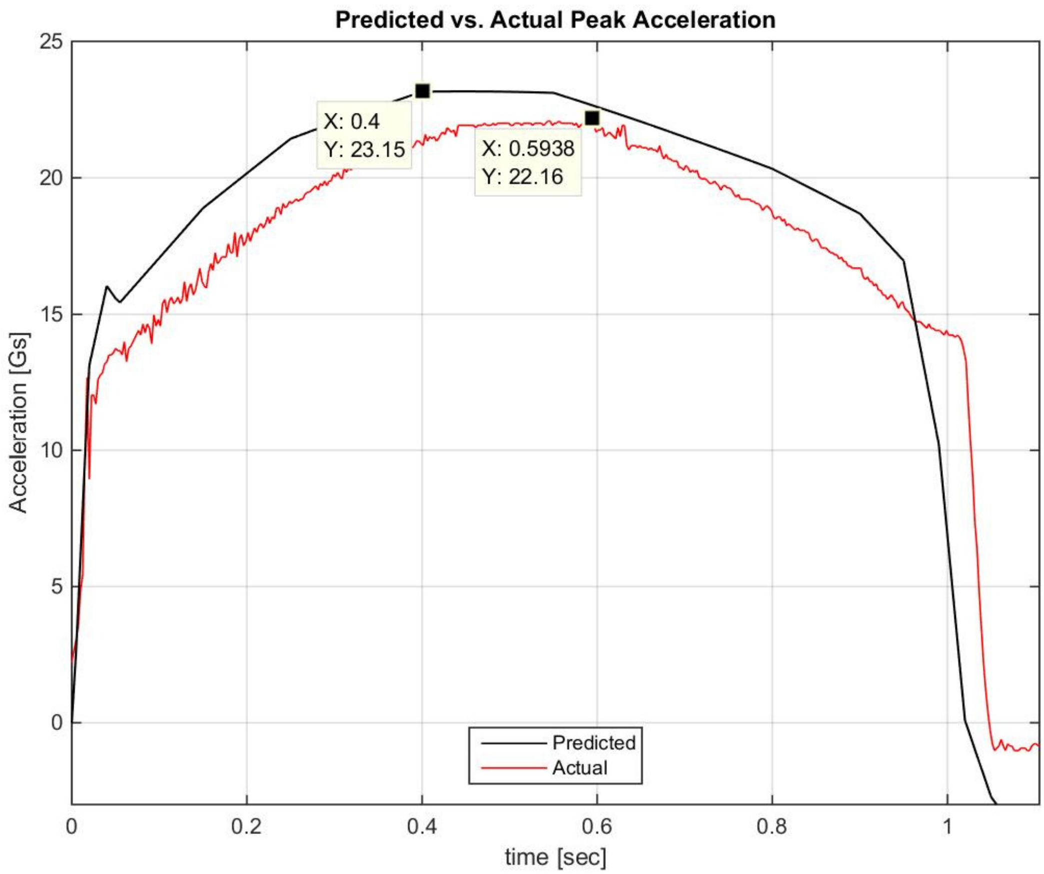

Figure 3. Acceleration curve of the boosted-dart combination during the coasting phase.

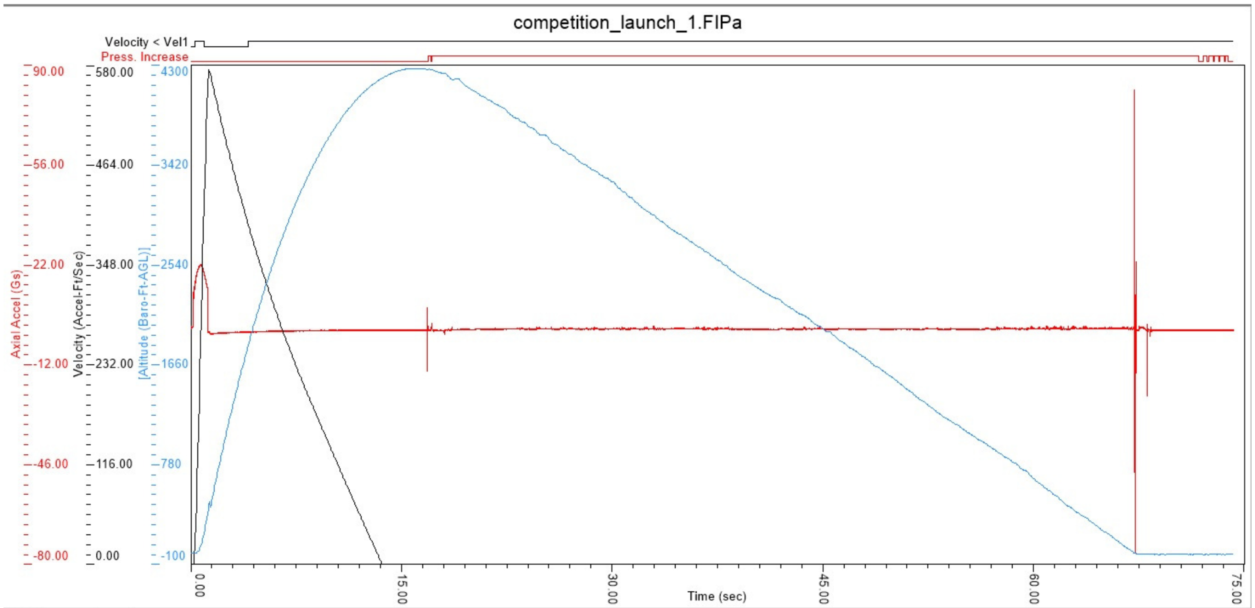

Figure 4. Raw data of dart trajectory taken from Raven3 altimeter. Above the graph, the Raven3 checks Boolean values before setting off the ejection charge. The graph indicates that the ejection charge was set off after apogee.

Data Collection

The first flight was successful in recording gyro sensor data from the 10-DOF sensor, but failed to capture video footage. The data shown in Figures 5, 6, and 7 were recorded in analog before converted to digital and, finally, converted to radians. The rotation data shown in Figures 6 and 7 were offset to 0 radians when aligned on the launch pad. The 3-axis rotation data was recorded up to the maximum altitude of the dart. The x-gyro shows that the dart was able to remain stable throughout its ascent while the y-gyro and z-gyro show that the dart was able to correct disturbances early in the boosting phase. There is minor oscillation in the transverse direction of the dart for the duration after burnout. This could be a result of its high static stability margin. A positive static margin will keep the dart stable, but if it is relatively large, then the dart may try to over correct disturbances.

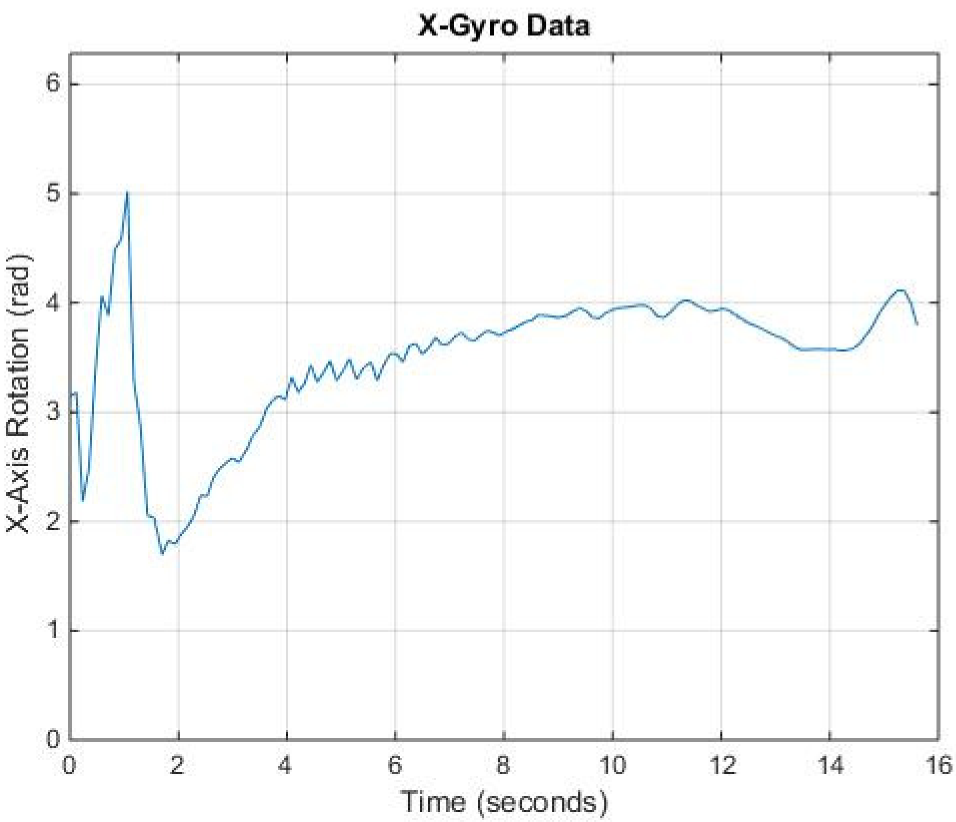

Figure 5. Rotation of the dart along the axial x-axis.

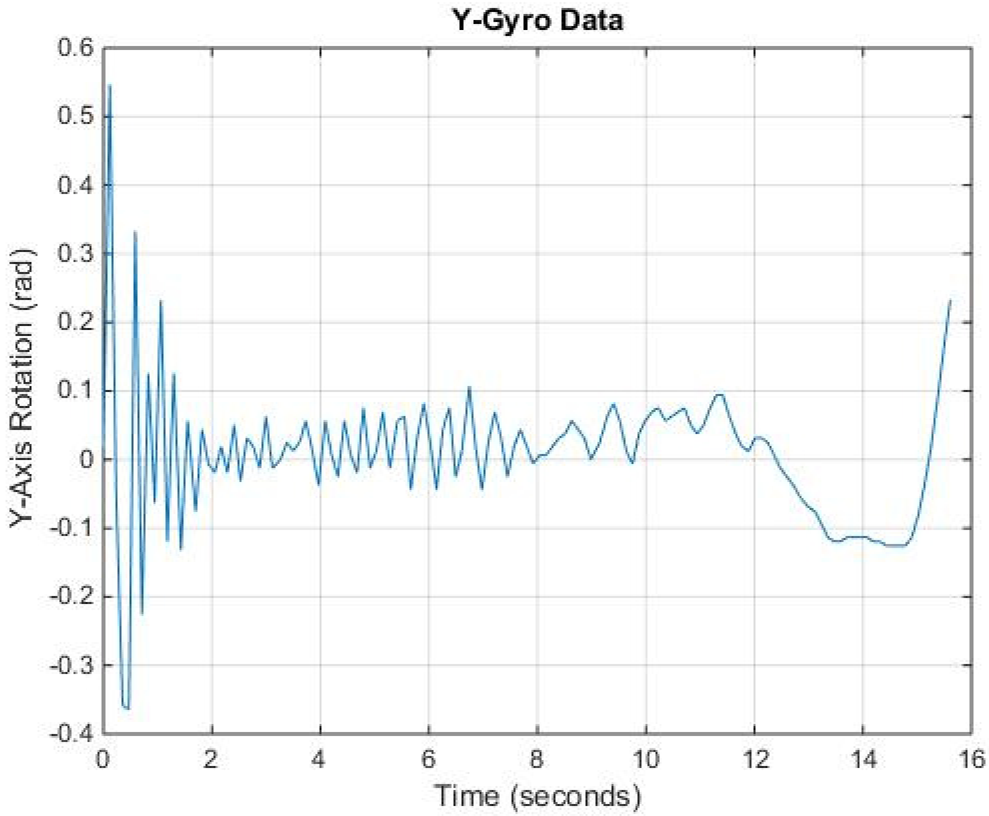

Figure 6. Rotation of the dart about the transverse y-axis.

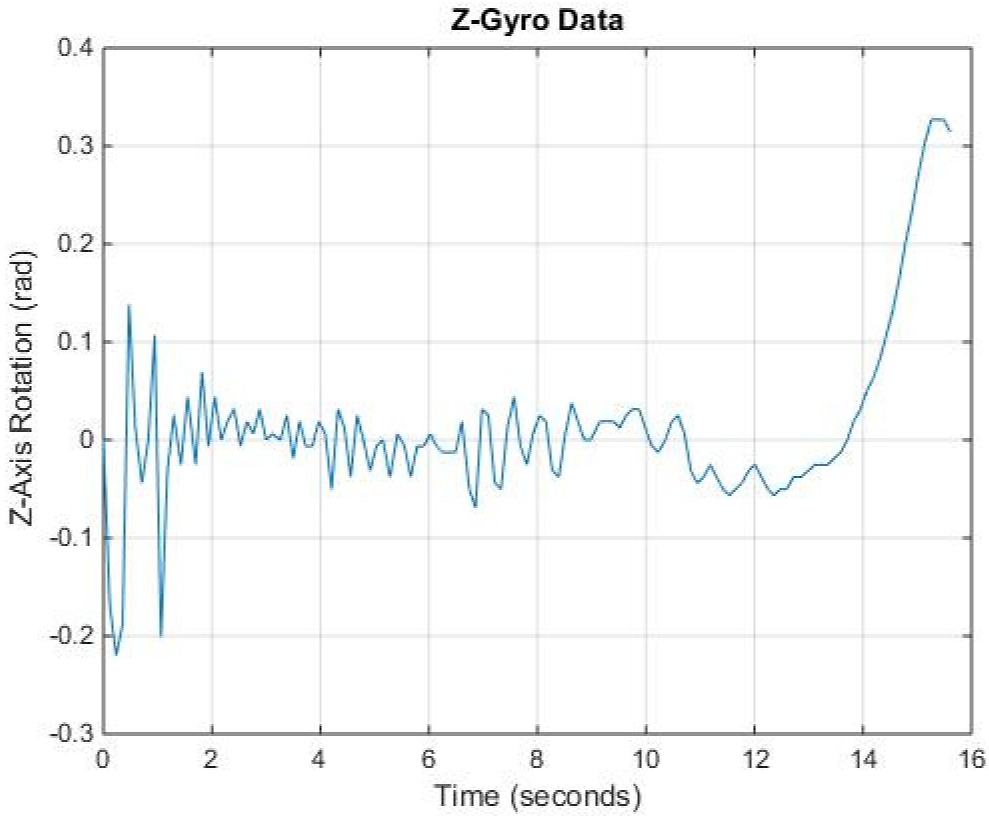

Figure 7. Rotation of the dart about the transverse z-axis.